RESEARCH ARTICLE

Flexible, Wearable and Fully-printed Smart Patch for pH and Hydration Sensing in Wounds

Mick Iversen, Monisha Monisha, Shweta Agarwala*

Department of Electrical and Computer Engineering, Finlandsgade 22, Aarhus University, Aarhus, Denmark

Abstract: Wound healing is a complex and dynamic regeneration process, wherein the physical and chemical parameters are continuously changing. Its management and monitoring can provide immense benefits, especially for bed-ridden patients. This work reports a low-cost, flexible, and fully printed on-skin patch sensor to measure the change in pH and fluid content in a wound. Such a bendable sensor can also be easily incorporated in a wound dressing. The sensor consists of different electrodes printed on polydimethylsiloxane (PDMS) substrate for pH and moisture sensing. The fabricated sensor patch has a sensitivity of 7.1 ohm/pH for wound pH levels. The hydration sensor results showed that moisture levels on a semi-porous surface can be quantified through resistance change.

Keywords: Smart patch; Wound management; pH sensor; Hydration sensor; Flexible electronics; Printed electronics

*Correspondence to: Shweta Agarwala, Department of Electrical and Computer Engineering, Finlandsgade 22, Aarhus University, Aarhus, Denmark; shweta@ece.au.dk

Received: September 30, 2021; **Accepted:** November 15, 2021; **Published Online:** December 16, 2021

(This article belongs to the *Special Section: 3D Printing and Bioprinting for the Future of Healthcare*)

Citation: Iversen M, Monisha M, Agarwala S, 2022, Flexible, Wearable and Fully-Printed Smart Patch for pH and Hydration Sensing in Wounds. *Int J Bioprint,* 8(1):447. http:// doi.org/10.18063/ijb.v8i1.447

1. Introduction

Wound management and its treatment have long been considered a problem for healthcare professionals[1]. Both acute and chronic wounds present a threat to global health and economy. Medical costs associated with wound care and treatments range from $28.1 billion to $96.8 billion due to a rise in aging population as well as the incidence of diabetes and obesity. There is a clear demand for more proactive responses that can manage, care or treat wounds and reduce the burden on healthcare resources[2].

Multifunctional flexible electronic devices have attracted attention owing to their potential applications in sustainable energy, smart displays, healthcare monitoring, wearables, human-machine interactions, soft robots, artificial skin, etc[3-7]. Among these wearable/on-body devices that are biocompatible and breathable are in huge demand due to their convenience and accessibility[8]. Ongoing research has shown that on-body flexible sensors can provide valuable information to help treat many ailments[9]. Despite the growing need, research progress on such devices is slow due to the complex device integration and lack of multifunctional nanomaterials.

There is a rise in demand for intelligent disposable patches that can provide timely and effective wound management through biochemical and physiological sensing, such as potential hydrogen (pH)[10,11], temperature[12,13], hydrogen peroxide[14,15], wound exudate volume[16], lactate[17,18], and glucose[19,20]. The pH level in a wound bed is a key indicative parameter for the assessment of the healing progress[21]. The pH of the wound is considered to be related to protease activity, angiogenesis, and bacterial infection, and therefore, continuous and real-time detection of pH is of great significance for monitoring wound healing[22]. Healthy skin is slightly acidic due to organic acid secretion of keratinocytes, secretions from sebaceous and sweat glands, and the pH fluctuates in alkaline range of 7-8 in unhealed wounds[23-28]. Exudate production is also important for the healing process to keep the wound moist, thereby allowing free movement of the epithelial cells.

There has been some work done in fabricating pH-sensing wound patches based on fibre optics[29], ion-sensitive field-effect transistor[30], nuclear magnetic resonance[31], Ultraviolet-visible spectroscopy[32,33], near-infrared spectroscopy[34], Raman spectroscopy[35,36], potentiometric sensor[37], pH-responsive dyes and quantum dots[38-48]. Despite the efforts, there are limitations of reliability, limited pH range, low sensitivity, complex design, autofluorescence, use of toxic dyes, and high production cost. Therefore, there exists a need to develop an easy-to-apply, non-toxic and low-cost system, which can quantify both wound exudate and pH levels in a wound.

This work demonstrates the potential of flexible and printed electronics for integrated wound monitoring by engineering an on-skin platform. The approach adopted in this work was based on the development of printed on-skin sensor patch, which can provide a simple result for the pH of the wound fluid. Single-walled carbon nanotubes (SWCNT) were used for pH sensing owing to their excellent sensitivity. In earlier reported work, a composite of carbon nanotubes (CNT) conductive polymers were used to increase the sensitivity but required the use of reference electrode, which is known to suffer from leakage of electrolyte[49,50]. Here, the change in CNT resistance is measured as a function of H^+ ion concentration without the requirement for a reference electrode[51,52]. The patches are also capable of stimulating the wound electrically for direct wound management using hydration sensing mechanism. Fabricated multifunctional patches show satisfactory repeatability, reusability, and response performance. To the authors knowledge, this is the first report on combining the two functionalities of pH and hydration sensing in a single patch for wound management. We have used the printing route to fabricate the wound patch due to its attractive features of low cost, material saving, and fast processing. Printed technologies are a fast-growing area with many techniques under its umbrella namely, material jetting, vat polymerization, and material extrusion[53-55]. We have chosen material extrusion as the preferred mode of printing due to the range of the viscosity of the materials used in this work. Material extrusion is also promising to create planar platforms with multi-material printing.

2. Materials and methods

2.1. Finite element analysis (FEA) simulation

Solidworks 2019 – 2020 student edition was used for the simulations of all models (**Figure S1**). Same forces and fixtures were applied to all models. Patches were subjected to forces in two directions: horizontal and vertical, as marked by yellow and green colored bars. It was found that the patch type II has the largest reduction of stress, and the shape was used to fabricate the wound patch in this work.

2.2. Fabrication of patch

Firstly, the substrate was fabricated according to the stimulated design. For this purpose, polydimethylsiloxane (PDMS) (Sylgard 184, DOW, Diatom, Denmark) was used and mixed with a curing agent (10:1 ratio) to give a solution with viscosity ~3.5 Pa.s. To adjust the viscosity of the solution, silicon dioxide nanoparticles (SiO_2 NPs) (5 – 20 nm, Merck Life Science, Denmark) were added in different ratios (**Figure S2**). The mixture was heated at 80°C for 10 min to get a homogenous solution. To remove trapped air and bubbles, solution was centrifuged at 6000 rpm for 10 min followed by degassing at 50°C. The patch was printed using Celllink's BIOX bioprinter with a mixture containing 20 wt% NPs. Substrate and top layer were printed using nozzle size and pressure of 22 G, 110 kPa and 25 G, 190 kPa, respectively, and a speed of 8 mm/s. Ag ink (Smart Fabric Ink tc-c4007, TC) was used for printing electrodes and hydration sensor. Printing was performed using nozzle size of 25 G with speed and pressure of 5 mm/s and 200 kPa, respectively. The temperature of printbed was kept at 60°C. The pH sensor was fabricated by printing SWCNT aqueous ink, (0.2 mg/mL, Merck Life Science, Denmark) using an inkjet printhead. A total of 30 layers were printed for homogeneity and interconnection between SWCNTs with a speed and pressure of 8 mm/s and 13 kPa, respectively. Valve open and cycle time was 1 ms and 100 ms, respectively. The temperature of the printbed was kept as 60°C with a curing time of 60 s. The complete fabrication process is depicted in **Figure 1**.

The complete patches were designed with four printed layers of PDMS modified with SiO_2 NPs as substrate material and commercial Ag and SWCNT inks (**Figure 1H**). Components 1-4 and 6 were printed and collectively called as patch while components five, seven, and eight were used as attachments to carry out the measurements without interfering with the printed parts. Top insulated layer (1 of **Figure 1H**) was designed to support the structure. The presence of three pockets allows easy access of fluid for pH and hydration sensors (2 and 4 of **Figure 1H**).

2.3. Resistance detection in buffer solution with different pH

Patches were tested in a buffer solution (McIlvaine buffer, Merck Life Science) and resistance change was measured with a digital Keithley model 2110. The sensor output was recorded using Kickstart (version 2.4) software. The sampling rate was 1 kHz, and the data was reviewed with the software KickStart 2. The patches

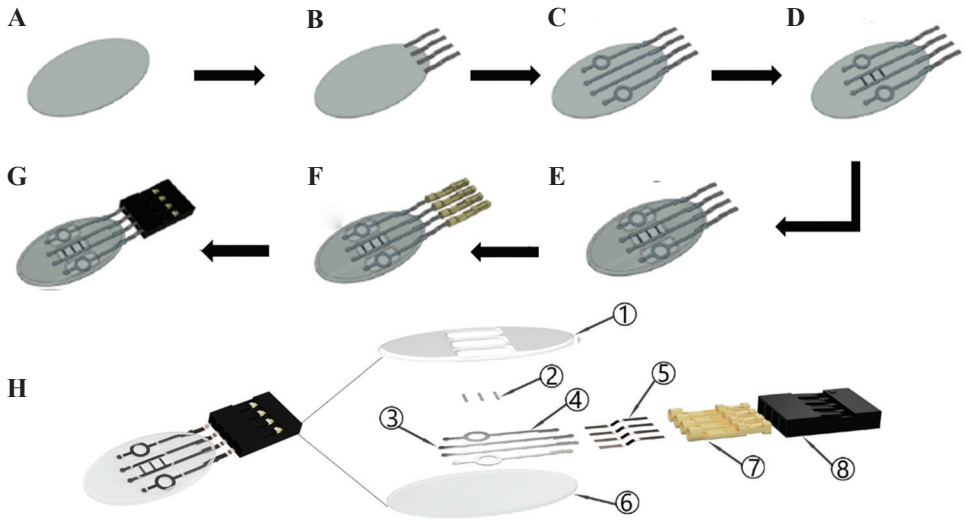

Figure 1. Schematic depicting the fabrication process of the on-skin patch using BIOX printer: (A) printed polydimethylsiloxane substrate, (B) attachment of copper sheet wires, (C) printing of Ag electrodes, (D) printing Single-walled carbon nanotubes for pH sensing, (E) printing of encapsulation layer, (F) connecting female pins and (G) connecting the socket to the copper sheet wires. (H) Exploded view of the patch with printed components.

were kept in the buffer solution until the measured resistance obtained a steady state, after which they were transferred to another buffer solution with a different pH. The buffer cycle followed the change from pH 9.18 – 6.86 – 4 – 6.86 – 9.18. To measure the sensitivity of the fabricated sensor, similar method was employed except that the pH of buffer solutions used were 5.8, 6.2, 6.6, 7, 7.7 and 7.8.

2.4. Hydration sensor

To measure the change in the resistance, patch was placed on a hotplate at 37°C to simulate normal skin temperature. A piece of fabric was placed onto the patch to avoid pre-load. A total of 300 µL (3 × 100 µL) of a buffer solution with a pH of 6.86 was dropped on the fabric at different intervals in a span of 15 min.

2.5. Repeatability

The patch was continuously shifted 12 times between buffer of pH 4 and 6.86 over 90 min to obtain resistance versus time plot.

2.6. Response time

Data of resistance detection in buffer solution with different pH were used to find out the response time by calculating the mean time taken to stabilize the patch on changing the pH.

2.7. Sensitivity

Sensitivity was calculated using two equations given below:

$$Sensitivity = \frac{\Omega}{pH}$$

$$Sensitivity = \frac{mV}{pH}$$

2.8. Offset drift

The patch was submerged in a beaker filled up to ¾ of buffer solution with pH 6.82 for 8 days. The beaker was sealed off with parafilm to prevent evaporation of buffer and measurement was taken once in a day.

3. Results and discussion

3.1. FEA results

FEA simulations were performed to investigate the stress around a wound when a load was applied to the skin. The central idea was to observe the effect of patch shape on the stress around the wound site. Reduced stress in a wound is crucial to lower the potential of fracturing a wound, thereby reducing the healing time. Wounds are reported to heal about 3 times faster in absence of any mechanical stress[56,57]. Further, it reduces the chances of reinfection[58]. Shape of the type II patch was found to relieve the maximum stress applied on the skin with a reduction of 66% (**Figure S1**). Oval shape of type II patch distributed the stress over a large area as indicated by lighter blue color in **Figure S3** and reduced the maximum stress at the narrowest points of the wound.

3.2. pH sensor and characteristics

PDMS was chosen as substrate because of its mechanical and biocompatibility properties. However, there is a downside of using PDMS as a substrate due to its hydrophobic properties, which impede the printing of SWCNT. The presence of metal in nano-form or introduction of silano group is known to introduce hydrophilicity in PDMS[59]. Hence, SiO_2 NPs were introduced in PDMS to make it hydrophilic. Incorporation of SiO_2 in PDMS allows the material composite to be more viscous and be cured in desired shape through the formation of an interconnected three-dimensional (3D) network within. The printed patch with all components is shown in **Figure 2A**. SEM analysis of the printed SWCNT layers reveals that the printing was homogeneous without voids. The observed cracks are due to handling of the sample.

Both acute and chronic wounds experience pH values between 7.15 and 8.9. The main difference lies in the time window for healing, wherein a chronic wound takes more than a week to heal[10,60]. In general, a wound with pH in the range 5.4 – 7.3 is considered in the proliferation phase and not categorized as a chronic wound. A sensitive pH sensor should thus successfully measure the pH range of 5.4 – 8.9. It is reported that the electrical resistance of SWCNT decreases in acidic solutions with increase in potential and vice visa for alkaline solutions[11,52]. Thus, the change in conductivity for SWCNTs depends on the pH value[61]. For this reason, SWCNT inks were utilized as non-toxic material to fabricate a pH sensor. **Figure 3A** and **S4a** show the change of resistance and mean of three runs with respect to time for the fabricated patch, respectively. The working of the patch was tested in pHHH cycle of 9.18 – 6.86 – 4 – 6.86 and back to 9.18. The results were found to be consistent for all the runs throughout the cycle. Further, the sensitivity of same patch was measured in the pH range of 5.8 – 7.8. The results are shown in **Figure 3B** with a plot of mean values for run 2 – 5 is represented in **Figure S4b**. Except for the first run, the results were consistent in the complete cycles. The discrepancy in the first run may be attributed to the dried-out buffer solution on the electrodes from the previous studies. The considerable difference in the resistance between buffer solutions corresponds to better sensitivity.

Repeatability is defined as the sensor's capability to provide same results under same circumstances. The repeatability of the fabricated sensor is plotted in **Figure 4A**, where change in resistance was observed with time. The maximum difference between the first maximum and minimum resistance values was found to be 0.9. **Figure 4B** shows the response time of the fabricated sensor when subjected to different buffer solutions. The

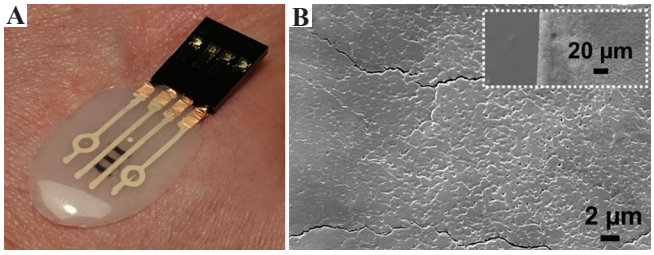

Figure 2. (A) Fabricated patch with polydimethylsiloxane substrate containing 20 wt% of SiO2 NPs and Ag and single-walled carbon nanotubes (SWCNT) electrodes and (B) SEM image showing the surface of printed SWCNT material. The inset depicts the interface between polydimethylsiloxane (darker region) and SWCNTs.

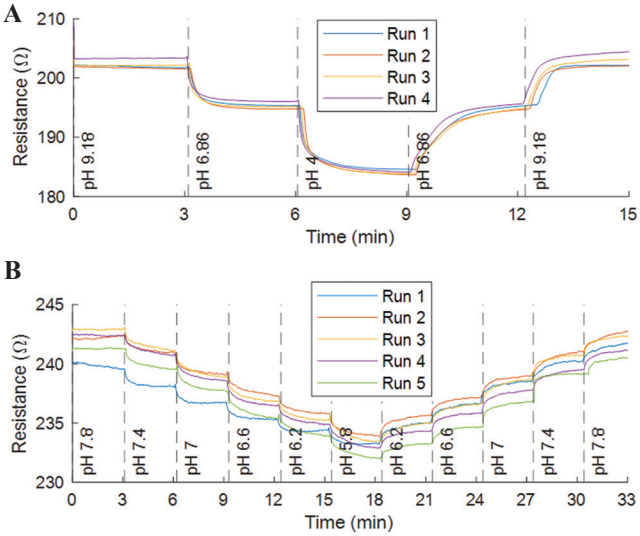

Figure 3. Measured resistance for different buffer solutions with 3 min intervals.

fastest response time was recorded at ~56 s when the buffer solution changed from pH 9.18 to pH 6.56 and the slowest at ~134 s when measured for solution from pH 4 to 6.86. The mean response time was calculated to be ~92 s. It was observed that the response time was longer when measuring from acidic to alkaline solutions than vice versa, and can be explained by the lower concentration of hydrogen ions in more alkaline buffer where the protonation and deprotonation process becomes slower[62].

Sensitivity is defined as the slope of the transfer function of the sensor and is a measure of the magnitude of the output response to the sensor input. The fabricated sensor was tested for sensitivity in the pH ranges of 4 – 9.18 and 5.2 – 7.8, where the highest sensitivity for each range was recorded to be 4.1/pH and 7.4/pH, respectively. It is also reported in the literature that the sensitivity varies with the number of printed layers[11] and with decrease in the effective surface area[52]. However, the precision value for the sensor was found to be ~0.7 pH, which renders the patch effective to determine the

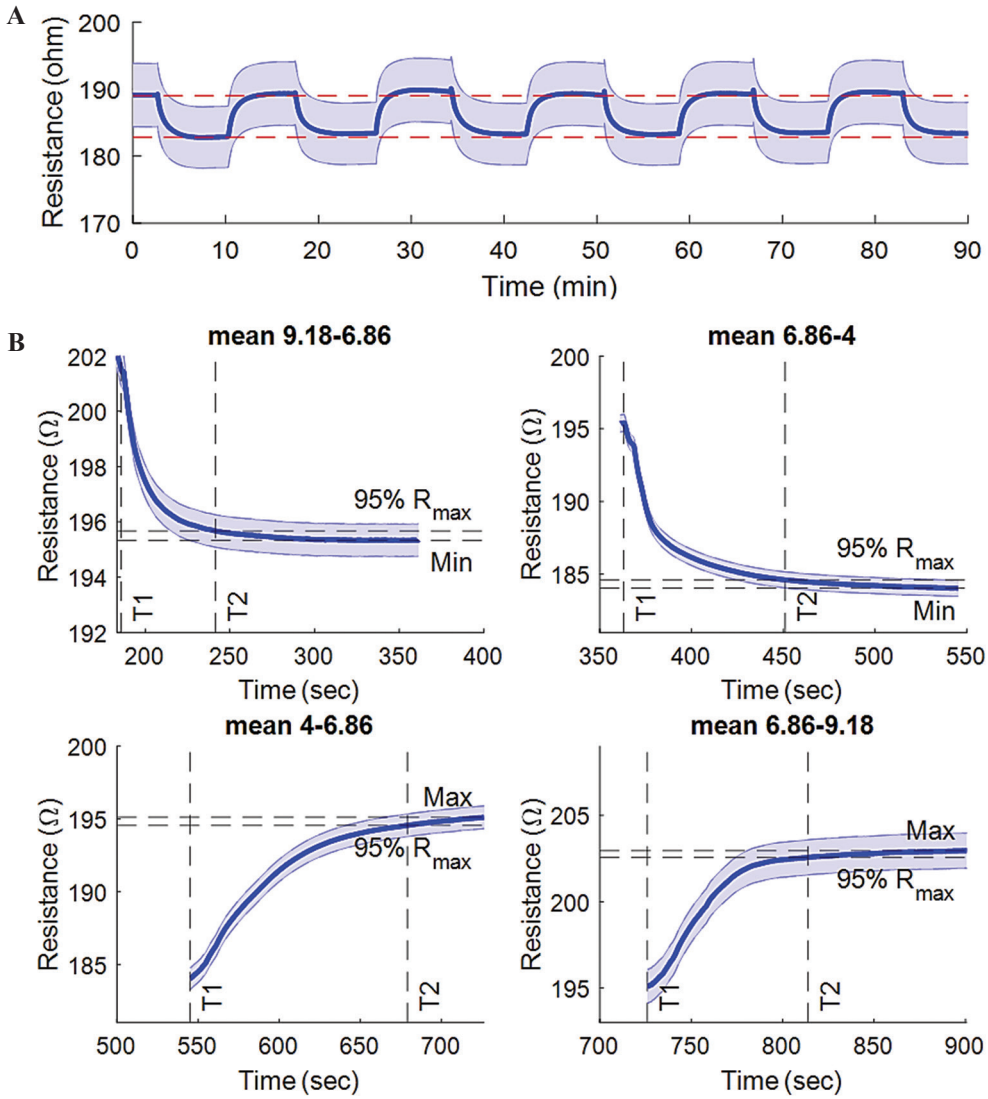

Figure 4. (A) Repeatability and (B) response time plot displaying resistance versus time, for two buffers with pH 4 and 6.86.

state of the wound. This patch is particularly suited for chronic wounds where the pH tends to be above 8.

Hysteresis, which indicates the degree of inconsistency between the increasing and reverse loading, was also tested. For a more detailed description of the hysteresis, data points from **Figure 3** were chosen. In **Figure 5A**, a hysteresis plot can be seen, where the maximum difference was found to be 0.2, and this related to 1% of the measured resistance range. **Figure 5B** shows the hysteresis plot where the pH range found in wounds have been used, and the maximum difference was 1.6, thus relating to 10% of the resistance range.

3.3. Hydration sensor

Wound exudate mainly consists of water and has high protein content[63]. The amount of exudate affects the healing process in wounds. With the fabricated sensors, the hydration (or fluid) level can be detected with respect to the measured resistance of the sensor ranging from 0 to 100%. As can be seen from **Figure 6**, there was a noticeable change in the resistance pertaining to the uptake of the fluids (buffer solution of pH 6.86 added to the fabric) by the sensor. At 100% hydration, the samples were saturated with resistance values of 300 – 400 kΩ. The samples were then left undisturbed, wherein the fluids started to evaporate. At the semi-dry state, we observed the resistance value to shoot up to 6000 – 7000 kΩ. The resistance further increased to 12,000 – 13,000 kΩ when completely dried. All the samples were consistent in the measured resistance values, where the slight variation happened in the time to reach from fully hydrated to the dry state.

When measuring the hydration, with direct current (DC), the resistance varied with the change in variables depending on the wound condition. Thus, the

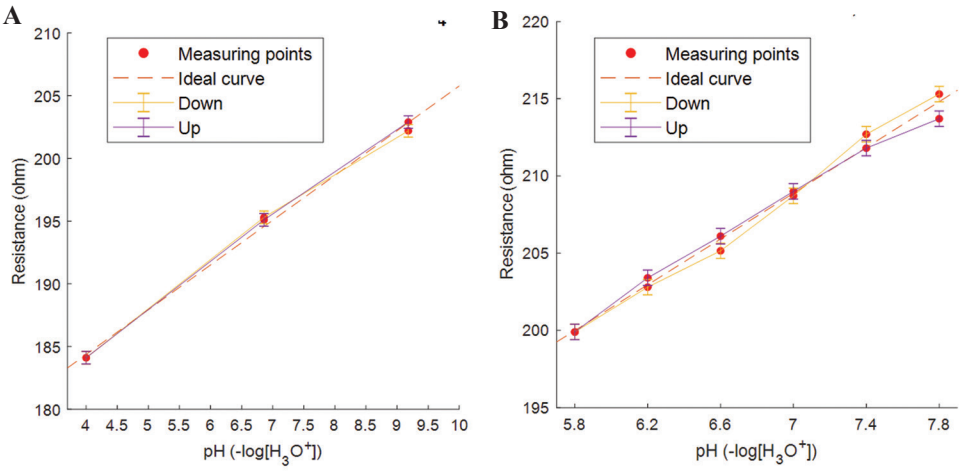

Figure 5. Hysteresis plot (A) and (B) made by using mean data points of Figure S4a and S4b, respectively.

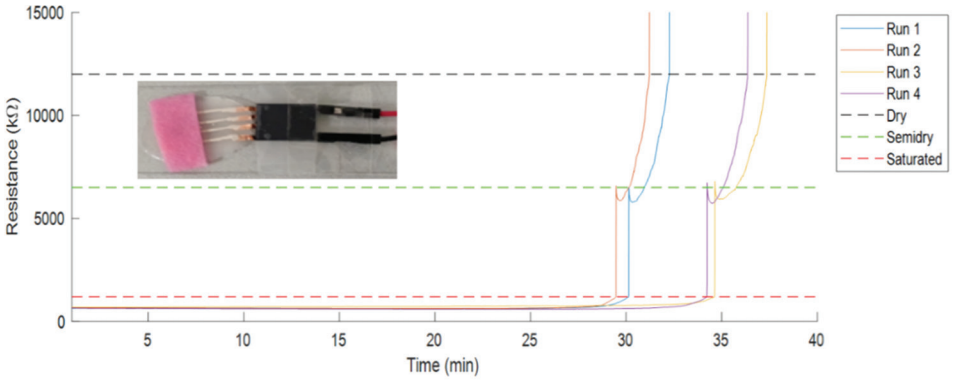

Figure 6. Resistance versus time plots indicating change in hydration.

resistance depends on below equations with change in fluid content and surface area of electrodes in contact with the fluid.

$$R = \frac{U}{I} \quad (1)$$

$$R = \rho \frac{L}{A} \quad (2)$$

where R = eesistance (Ω), U = voltage (V), I = current (A), ρ= resistivity (Ω m), L = length between electrodes (m), and A = surface area of electrodes (m^2).

The sensor patch was fabricated for the purpose of validating the measurements for wound management. The hydration sensor gives an indication of the presence of fluid in the wound, and if that is true, the measurements of the pH sensor originate from the wound fluid and not the dried-out residue left on the pH sensor.

4. Conclusions

The work demonstrates the feasibility of fully printing a wound management patch. The wound patch was fabricated with the purpose of enhancing wound. The focus is to measure the health status of the wound through indicative pH and hydration levels in a single patch. A PDMS-based substrate was used to print SWCNT and silver functional inks as sensing elements. Inkjet printing was employed for the patch and optimized to get the desired design and dimensions. The fabricated sensor patch has a sensitivity of 7.1 ohm/pH for wound pH levels. The measured resistance changes suggested that the sensor is able to measure wound exudate and serve as detector for wound fluids. It was also concluded that the sensitivity and precision of the patch can be controlled by removal of excess SWCNTs and through the printing process.

Acknowledgments

This work was supported by the Dean Start-up grant, Science and Technology, Aarhus University, Denmark.

Conflict of interest

The authors declare no conflicts of interest.

Author contributions

M.I. and S.A. conceptualize and designed the overall experiments. M.I. performed the experiments and formal analysis. M.M. wrote the manuscript and performed review and editing with support from S.A. S.A. supervised the project and conceived the original idea.

References

1. Kathawala MH, Ng WL, Liu D, *et al.*, 2019, Healing of Chronic Wounds: An Update of Recent Developments and Future Possibilities. *Tissue Engineering Part B: Reviews*, 25:429–44. https://doi.org/10.1089/ten.TEB.2019.0019
2. Gianino E, Miller C, Gilmore J, 2018, Smart Wound Dressings for Diabetic Chronic Wounds. *Bioengineering*, 5:51. https://doi.org/10.3390/bioengineering5030051
3. Dubal DP, Chodankar NR, Kim DH, *et al.*, 2018, Towards Flexible Solid-state Supercapacitors for Smart and Wearable Electronics. *Chem Soc*, 47:2065–129. https://doi.org/10.1039/C7CS00505A
4. Lv T, Liu M, Zhu D, *et al.*, 2018, Nanocarbon-based Materials for Flexible All-solid-State Supercapacitors. *Adv Mater*, 30:1705489. https://doi.org/10.1002/adma.201705489
5. Weng W, Yang J, Zhang Y, *et al.*, 2020, A Route Toward Smart System Integration: From Fiber Design to Device Construction. *Adv Mater*, 32:1902301. https://doi.org/10.1002/adma.201902301
6. Chen Y, Pötschke P, Pionteck J, *et al.*, 2018, Smart Cellulose/Graphene Composites Fabricated by *In Situ* Chemical Reduction of Graphene Oxide for Multiple Sensing Applications. *J Mater Chem A*, 6:7777–85. https://doi.org/10.1039/C8TA00618K
7. Li Q, Zhang J, Li Q, *et al.*, 2019, Review of Printed Electrodes for Flexible Devices. *Front Mater*, 5:77. https://doi.org/10.3389/fmats.2018.00077
8. He T, Wang H, Wang J, *et al.*, 2019, Self-sustainable Wearable Textile Nano-energy Nano-system (NENS) for Next-generation Healthcare Applications. *Adv Sci*, 6:1901437. https://doi.org/10.1002/advs.201901437
9. Jin Y, Chen G, Lao K, *et al.*, 2020, Identifying Human Body States by Using a Flexible Integrated Sensor. *npj Flex Electron*, 4:1–8. https://doi.org/10.1038/s41528-020-00090-9
10. Schneider LA, Korber A, Grabbe S, *et al.*, 2007, Influence of pH on Wound-healing: A New Perspective for Wound-therapy? *Arch Dermatol*, 298:413–20. https://doi.org/10.1007/s00403-006-0713-x
11. Goh GL, Agarwala S, Tan YJ, *et al.*, 2018, A Low Cost and Flexible Carbon Nanotube pH Sensor Fabricated Using Aerosol Jet Technology for Live Cell Applications. *Sens Actuators B Chem*, 260:227–35. https://doi.org/10.1016/j.snb.2017.12.127
12. Armstrong DG, Lavery LA, Liswood PJ, *et al.*, 1997, Infrared Dermal Thermometry for the High-risk Diabetic Foot. *Phys Ther*, 77:169–75. https://doi.org/10.1093/ptj/77.2.169
13. Bharara M, Schoess J, Nouvong A, *et al.*, 2010, Wound Inflammatory Index: A "Proof of Concept" Study to Assess Wound Healing Trajectory. Thousand Oaks, California: SAGE Publications.
14. Liu X, Zweier JL, 2001, A Real-Time Electrochemical Technique for Measurement of Cellular Hydrogen Peroxide Generation and Consumption: Evaluation in Human Polymorphonuclear Leukocytes. *Free Radic Biol Med*, 31:894–901. https://doi.org/10.1016/s0891-5849(01)00665-7
15. Test ST, Weiss S, 1984, Quantitative and Temporal Characterization of the Extracellular H_2O_2 Pool Generated by Human Neutrophils. *J Biol Chem*, 259:399–405. https://doi.org/10.1016/s0021-9258(17)43674-x
16. McColl D, Cartlidge B, Connolly P, 2007, Real-Time Monitoring of Moisture Levels in Wound Dressings *In Vitro*: An Experimental Study. *Int J Surg*, 5:316–22. https://doi.org/10.1016/j.ijsu.2007.02.008
17. Cho M, Hunt TK, Hussain MZ, 2001, Hydrogen Peroxide Stimulates Macrophage Vascular Endothelial Growth Factor Release. *Am J Physiol Heart Circ Physiol*, 280:H2357–63. https://doi.org/10.1152/ajpheart.2001.280.5.H2357
18. Trabold O, Wagner S, Wicke C, *et al.*, 2003, Lactate and Oxygen Constitute a Fundamental Regulatory Mechanism in Wound Healing. *Wound Repair Regen*, 11:504–9. https://doi.org/10.1046/j.1524-475X.2003.11621.x
19. Lee H, Song C, Hong YS, *et al.*, 2017, Wearable/Disposable Sweat-based Glucose Monitoring Device with Multistage Transdermal Drug Delivery Module. *Sci Adv*, 3:e1601314. https://doi.org/10.1126/sciadv.1601314
20. Yu Y, Li P, Zhu C, *et al.*, 2019, Multifunctional and Recyclable Photothermally Responsive Cryogels as Efficient Platforms for Wound Healing. *Adv Funct Mater*, 29:1904402. https://doi.org/10.1002/adfm.201904402

21. Ninan N, Forget A, Shastri VP, *et al.*, 2016, Antibacterial and Anti-inflammatory pH-Responsive Tannic Acid-carboxylated Agarose Composite Hydrogels for Wound Healing. *ACS Appl Mater Interfaces*, 8:28511–21. https://doi.org/10.1021/acsami.6b10491
22. Piva RH, Rocha MC, Piva DH, *et al.*, 2018, Acidic Dressing Based on Agarose/CS_2. 5H0. 5PW12O40 Nanocomposite for Infection Control in Wound Care. *ACS Appl Mater Interfaces*, 10:30963–72. https://doi.org/10.1021/acsami.8b09066
23. Zlotogorski A, 1987, Distribution of Skin Surface pH on the Forehead and Cheek of Adults. *Arch Dermatol*, 279:398–401. https://doi.org/10.1007/BF00412626
24. Dargaville TR, Farrugia BL, Broadbent JA, *et al.*, 2013, Sensors and Imaging for Wound Healing: A Review. *Biosens Bioelectron*, 41:30–42. https://doi.org/10.1016/j.bios.2012.09.029
25. Schmid-Wendtner MH, Korting HC, 2006, The pH of the Skin Surface and its Impact on the Barrier Function. *Skin Pharmacol Physiol*, 19:296–302. https://doi.org/10.1159/000094670
26. Ehlers C, Ivens U, Møller M, *et al.*, 2001, Comparison of Two pH Meters Used for Skin Surface pH Measurement: The pH Meter "pH900" from Courage and Khazaka Versus the pH Meter "1140" from Mettler Toledo. *Skin Res Technol*, 7:84–9. https://doi.org/10.1034/j.1600-0846.2001.70205.x
27. Wang M, Wang C, Chen M, *et al.*, 2019, Efficient Angiogenesis-based Diabetic Wound Healing/Skin Reconstruction through Bioactive Antibacterial Adhesive Ultraviolet Shielding Nanodressing with Exosome Release. *ACS Nano*, 13:10279–93. https://doi.org/10.1021/acsnano.9b03656
28. Jones EM, Cochrane CA, Percival SL, 2015, The Effect of pH on the Extracellular Matrix and Biofilms. *Adv Wound Care*, 4:431–9. https://doi.org/10.1089/wound.2014.0538
29. Baldini F, Bechi P, Bracci S, *et al.*, 1995, *In Vivo* Optical-Fibre pH Sensor for Gastro-Oesophageal Measurements. *Sens Actuators B Chem*, 29:164–8. https://doi.org/10.1016/0925-4005(95)01678-3
30. Sudakov-Boreysha L, Dinnar U, Nemirovsky Y, 2004, New ISFET Catheters Encapsulation Techniques for Brain PH *In-Vivo* Monitoring, Proceedings of the 2004 11th IEEE International Conference on Electronics, Circuits and Systems. ICECS, p424-426.
31. Yoshioka Y, Oikawa H, Ehara S, *et al.*, 2002, Noninvasive Estimation of Temperature and pH in Human Lower Leg Muscles Using 1H Nuclear Magnetic Resonance Spectroscopy. *Spectroscopy*, 16:183–90. https://doi.org/10.1155/2002/392987
32. Pietsch C, Hoogenboom R, Schubert US, 2009, Soluble Polymeric Dual Sensor for Temperature and pH Value. *Angew Chem*, 121:5763–6. https://doi.org/10.1002/anie.200901071
33. Safavi A, Abdollahi H, 1998, Optical Sensor for High pH Values. *Anal Chim Acta*, 367:167–73. https://doi.org/10.1016/S0003-2670(98)00079-8
34. Soyemi O, Shear M, Landry M, *et al.*, 2005, *In Vivo* Noninvasive Measurement of Muscle pH during Exercise Using Near-infrared Spectroscopy, Smart Medical and Biomedical Sensor Technology III, International Society for Optics and Photonics, 60070N.
35. Van der Schueren L, De Clerck K, 2010, The Use of pH-Indicator Dyes for pH-Sensitive Textile Materials. *Text Res J*, 80:590–603. https://doi.org/10.1177/0040517509346443
36. Shoghi F, Mal S, Tie M, *et al.*, 2021, pH Responsive Platinum-Coated Single-Walled Carbon Nanotube Optical Sensor with Internal Reference. *Carbon*, 184:659–68. https://doi.org/10.1016/j.carbon.2021.08.065
37. Guinovart T, Valdés-Ramírez G, Windmiller JR, *et al.*, 2014, Bandage-based Wearable Potentiometric Sensor for Monitoring Wound pH. *Electroanalysis*, 26:1345–53. https://doi.org/10.1002/elan.201300558
38. Arafat MT, Mahmud MM, Wong SY, *et al.*, 2021, PVA/PAA Based Electrospun Nanofibers with pH-responsive Color Change Using Bromothymol Blue and on-Demand Ciprofloxacin Release Properties. *J Drug Deliv Sci Technol*, 61:102297. https://doi.org/10.1016/j.jddst.2020.102297
39. Bazbouz MB, Tronci G, 2019, Two-layer Electrospun System Enabling Wound Exudate Management and Visual Infection Response. *Sensors*, 19:991. https://doi.org/10.3390/s19050991
40. Tamayol A, Akbari M, Zilberman Y, *et al.*, 2016, pH-Sensing Hydrogel Fibers: Flexible pH-Sensing Hydrogel Fibers for Epidermal Applications. *Adv Healthc Mater*, 5:711–9. https://doi.org/10.1002/adhm.201500553
41. Mirani B, Pagan E, Currie B, *et al.*, 2017, An Advanced Multifunctional Hydrogel-Based Dressing for Wound Monitoring and Drug Delivery. *Adv Healthc Mater*, 6:1700718. https://doi.org/10.1002/adhm.201700718
42. Yang P, Zhu Z, Zhang T, *et al.*, 2019, Orange-Emissive Carbon Quantum Dots: Toward Application in Wound pH Monitoring

Based on Colorimetric and Fluorescent Changing. *Small*, 15:1902823.
https://doi.org/10.1002/smll.201902823

43. Begu S, Mordon SR, Desmettre T, *et al.*, 2005, Fluorescence Imaging Method for *In Vivo* pH Monitoring during Liposomes Uptake in Rat Liver Using a pH-Sensitive Fluorescent Dye. *J Biomed Opt*, 10:024008.
https://doi.org/10.1117/1.1899685
44. Malkaj P, Dalas E, Vitoratos E, *et al.*, 2006, pH Electrodes Constructed from Polyaniline/Zeolite and Polypyrrole/Zeolite Conductive Blends. *J Appl Polym Sci*, 101:1853–6.
https://doi.org/10.1002/app.23590
45. Trupp S, Alberti M, Carofiglio T, *et al.*, 2010, Development of pH-Sensitive Indicator Dyes for the Preparation of Micro-patterned Optical Sensor Layers. *Sens Actuators B Chem*, 150:206–10.
https://doi.org/10.1016/j.snb.2010.07.015
46. Mohr GJ, Müller H, Bussemer B, *et al.*, 2008, Design of Acidochromic Dyes for Facile Preparation of pH Sensor Layers. *Anal Bioanal Chem*, 392:1411–8.
https://doi.org/10.1007/s00216-008-2428-7
47. Yuan F, Ding L, Li Y, *et al.*, 2015, Multicolor Fluorescent Graphene Quantum Dots Colorimetrically Responsive to All-pH and a Wide Temperature Range. *Nanoscale*, 7:11727–33.
https://doi.org/10.1039/C5NR02007G
48. Wang L, Li M, Li W, *et al.*, 2018, Rationally Designed Efficient Dual-Mode Colorimetric/Fluorescence Sensor Based on Carbon Dots for Detection of pH and Cu^{2+} Ions. *ACS Sustain Chem Eng*, 6:12668–74.
https://doi.org/10.1021/acssuschemeng.8b01625
49. Ferrer-Anglada N, Kaempgen M, Roth S, 2006, Transparent and Flexible Carbon Nanotube/Polypyrrole and Carbon Nanotube/Polyaniline pH Sensors. *Phys Status Solidi B*, 243:3519–23.
https://doi.org/10.1002/pssb.200669220
50. Liao Y, Zhang C, Zhang Y, *et al.*, 2011, Carbon Nanotube/Polyaniline Composite Nanofibers: Facile Synthesis and Chemosensors. *Nano Lett*, 11:954–9.
https://doi.org/10.1021/nl103322b
51. Gou P, Kraut ND, Feigel IM, *et al.*, 2014, Carbon Nanotube Chemiresistor for Wireless pH Sensing. *Sci Rep*, 4:1–6.
https://doi.org/10.1038/srep04468
52. Qin Y, Kwon HJ, Subrahmanyam A, *et al.*, 2016, Inkjet-printed Bifunctional Carbon Nanotubes for pH Sensing. *Mater Lett*, 176:68–70.
https://doi.org/10.1016/j.matlet.2016.04.048
53. Jiang T, Munguia-Lopez JG, Flores-Torres S, *et al.*, 2019, Extrusion Bioprinting of Soft Materials: An Emerging Technique for Biological Model Fabrication. *Appl Phys Rev*, 6:011310.
https://doi.org/10.1063/1.5059393
54. Li X, Liu B, Pei B, *et al.*, 2020, Inkjet Bioprinting of Biomaterials. *Chem Rev*, 120:10793–833.
doi.org/10.1021/acs.chemrev.0c00008
55. Ng WL, Lee JM, Zhou M, *et al.*, 2020, Vat Polymerization-based Bioprinting Process, Materials, Applications and Regulatory Challenges. *Biofabrication*, 12:022001.
doi.org/10.1088/1758-5090/ab6034
56. Cremers NA, Suttorp M, Gerritsen MM, *et al.*, 2015, Mechanical Stress Changes the Complex Interplay between HO-1, Inflammation and Fibrosis, during Excisional Wound Repair. *Front Med*, 2:86.
https://doi.org/10.3389/fmed.2015.00086
57. Barnes LA, Marshall CD, Leavitt T, *et al.*, 2018, Mechanical Forces in Cutaneous Wound Healing: Emerging Therapies to Minimize Scar Formation. *Adv Wound Care*, 7:47–56.
https://doi.org/10.1089/wound.2016.0709
58. Urschel J, Scott P, Williams H, 1988, The Effect of Mechanical Stress on Soft and Hard Tissue Repair; a Review. *Br J Plast Surg*, 41:182–6.
https://doi.org/10.1016/0007-1226(88)90049-5
59. Liang FC, Chang YW, Kuo CC, *et al.*, 2019, A Mechanically Robust Silver Nanowire Polydimethylsiloxane Electrode Based on Facile Transfer Printing Techniques for Wearable Displays. *Nanoscale*, 11:1520–30.
https://doi.org/10.1039/C8NR08819E
60. Boateng J, 2020, Therapeutic Dressings and Wound Healing Applications. New York: John Wiley and Sons.
61. Lee D, Cui T, 2009, pH-dependent Conductance Behaviors of Layer-by-layer Self-Assembled Carboxylated Carbon Nanotube Multilayer Thin-film Sensors. *J Vac Sci Technol B*, 27:842–8.
https://doi.org/10.1116/1.3002386
62. Li P, Martin CM, Yeung KK, *et al.*, 2011, Dielectrophoresis Aligned Single-walled Carbon Nanotubes as pH Sensors. *Biosensors*, 1:23–35.
https://doi.org/10.3390/bios1010023
63. Cutting KF, 2003, Wound Exudate: Composition and Functions. *Br J Community Nurs*, 8 Suppl 3:S4–9.
https://doi.org/10.12968/bjcn.2003.8.sup3.11577

Publisher's note